Biomass Conversion and Biorefinery
https://doi.org/10.1007/s13399-023-04693-w

ORIGINAL ARTICLE

Adsorption of gas-styrene on activated carbon from agro-waste of *Silybum marianum* L. as a sustainable precursor

Kaan Isinkaralar[1] · Kulzira Mamyrbayeva[2] · Ahmad Hosseini-Bandegharaei[3]

Received: 23 May 2023 / Revised: 25 July 2023 / Accepted: 26 July 2023
© The Author(s), under exclusive licence to Springer-Verlag GmbH Germany, part of Springer Nature 2023

Abstract

Styrene adsorption has always been a research focus in the field of the gas environment due to its widespread usage. Removal of styrene using activated carbon has been verified because of the physicochemical properties of SMACs prepared by activating *Silybum marianum* L. waste powder. Hence, a series of novel SMACs were synthesized from NaOH, KOH, and H_3PO_4 ratio of 1:1–5 w/w and pyrolyzing at 450–950 °C and then washed activated carbon with HCl and NaOH. SMAC82, SMAC137, and the optimal AC (SMAC249) had the largest styrene adsorption capacity, 229, 170, and 136 mg/g for 700 ppm of styrene. Styrene is a typical model for volatile organic compounds (VOCs) in the atmosphere, and the findings demonstrated that it is rapidly absorbed into SMAC82, SMAC137, and SMAC249 through strong physical sorption. The calculated adsorption amounts showed that the styrene capture processes were feasible for adsorption within a suitable contact time and with excellent equilibrium adsorption capacities. Also, the results showed that the highest removal efficiency at 25 °C by the adsorption of SMAC82, SMAC137, and SMAC249 was 92%, 88%, and 86%, respectively. The efficiency results of SMAC82, SMAC137, and SMAC249 show that the styrene breakthrough at 25 °C compared to that of 35 and 45 °C increases approximately two times. Overall, this SMAC82 presented an excellent separation performance for styrene removal and can be a potential option for industrial applications of other VOCs in gas-phase, indicating good adsorption ability.

Keywords Adsorption process · Gaseous styrene · Microporous activated carbon · VOC treatment

1 Introduction

Industry development has created volatile organic compound (VOC) emissions that have become progressively worse at the global and regional levels [1]. Today, the widespread use of chemicals in human life has led to environmental and human health problems. Air quality in workplaces has emerged in recent years as public health concerns arising from the lack of adequate ventilation and air filtration following the growth of industries. It has been associated with various hazardous chemicals in the air, including VOCs [2]. Some VOCs' toxic and adverse health effects, such as benzene, 1,3-butadiene, and styrene, are globally produced as millions of tons, making them a widely known chemical worldwide. Styrene (C_8H_8) has been identified as conceivably carcinogenic in Group 2A by the International Agency for Research on Cancer [3] and the US National Toxicology Program (US NTP). It is derived from the catalytic dehydrogenation of ethylbenzene, which is reversible with unfavorable thermodynamics and natural emission sources [4, 5]. Styrene has undergone extensive toxicological research and potentially harms children's health. It is included in the list of Chemical of High Concern to Children in Washington, USA [6]. High occupational exposures to styrene (over 100 ppm in the air) have been displayed to bring about prenarcotic central nervous system depression with symptoms such as drowsiness, headache, and balance disorder. Significant absorption of styrene occurs by inhalation in the working environment, particularly in the pressed plastic industries. Styrene is also an environmental pollutant in small amounts of food [7], drink [8], tobacco smoke [9], 3-D printers [10], and exhaust gas [11]. More than 100,000 workers are exposed to European Union styrene. According to

✉ Kaan Isinkaralar
kisinkaralar@kastamonu.edu.tr

1 Department of Environmental Engineering, Faculty of Engineering and Architecture, Kastamonu University, 37150 Kastamonu, Türkiye

2 Department of Metallurgical Engineering, Satbayev University, 22a Satbaev Str., Almaty 050013, Kazakhstan

3 Faculty of Chemistry, Semnan University, Semnan, Iran

Published online: 04 August 2023

the differences in exposure to concentration levels, it causes eye, nose, throat, and lung irritation and damages the liver, kidneys, and central nervous system [12, 13]. It is also seen in asthma, respiratory symptoms, cardiovascular disease, and occupational cancer [14].

Styrene, included in VOCs, is one of the widely used aromatic organic solvents produced by the dehydrogenation of ethyl benzene during decomposition [15]. Over 90% of styrene is used to make thousands of everyday products, such as polystyrene polymers [16], rubber [17], plastics, paints [18], toys [19], and home appliance components [20]. In the typical operating environment, air levels are less than 10.0 ppm, except in some parts of the reinforced plastic industries, where concentrations of 20.0 ppm or higher are distinct. Employees may be exposed to hazardous chemicals if they do not follow safety instructions. Controlling volatile organic air toxic emissions from industrial plants has become crucial and expensive for chemical industries, especially small-scale ones, to meet increasingly stringent quality standards. The biotechnological route to combat air pollution is a promising area of research that can provide reliable, facile, and inexpensive technologies for air pollution prevention [21]. Also, thanks to increased attention from regulatory authorities, legislation controlling air pollutant emissions has increased, and treatment systems have emerged in recent years to operate and maintain styrene successfully [22]. Thus, the intense exposure of people to these compounds in various industries worldwide has increased the search for filtration-removal methods in the way they work and work environments. The main styrene removal methods have been widely studied biofilters [23], bioscrubbers [24], adsorption [25], membrane separation [26], non-thermal plasma catalysis [27], biotrickling filters [28], bioreactors [29], and applied successfully to eliminate styrene vapor from the air stream.

Adsorption is specially adequate and cost-effective for treating high volumes of waste gases having low styrene concentrations [30]. Adsorption can also be combined with plasma, oxidation, and other technologies to improve purification efficiency [31]. Activated carbon (AC) is an effective adsorbent that removes styrene [32]. The AC is relatively inexpensive and can be obtained from many sources. Still, ambient moisture interferes with adsorption technologies used for volatile organic compound removal, which can reduce the adsorption capacity of adsorbents [33]. The ACs, dubbed activated charcoals, are black carbon porous solid substances with high specific surface areas, reasonable pore size distributions, and high surface reactivities. It is an amorphous and non-graphitic microcrystalline with a turbostratic structure.

Furthermore, it is environmentally friendly because the contaminants are completely converted at low temperatures into non-hazardous final products [34]. It is more effective in a solid–gas medium than other adsorbents due to their high surface area available for mass transfer. Studies have shown that using lignin-containing ACs can best achieve the optimum removal of airborne pollutants by aromatic hydrocarbons [35, 36].

Herein, towards investing in the ability of the novel SMACs to remove styrene vapors, the adsorption scrutinizations were conducted to gather sufficient information for future macro-kinetic studies and valuable data for industrial application. Among the various lignin-based wastes available, *Silybum marianum* L. biomass is renewable, feasibly accessible, and especially abundant in nature. Disposing of the massive amount of *Silybum marianum* L. produces a severe problem in the spontaneous landscape areas of cities as they slowly and progressively create waste biomass. Therefore, this study was conducted by researchers to try their best to prepare SMACs as low-cost and environmentally friendly precursors. This paper presents three interesting adsorbents from the novelty viewpoint. Firstly, the paper revises the results of selected SMACs on applying adsorption methods for styrene; thus, it may be a good coordination ability. Secondly, morphological structures were investigated by a comparison procedure for evaluating the influence of surface functionalization with infrared FTIR (Fourier transform infrared), SEM (scanning electron microscopy), thermogravimetric analysis (TGA), and BET (Brunner-Emmett-Teller method). Thirdly, a simple tool for the preliminary selection of the adsorption behaviors of SMACs towards styrene from gaseous solution. Furthermore, the temperature and contact time were examined to compare styrene vapor.

2 Materials and methods

2.1 Preparation of activated carbons

To prepare the SMACs from *Silybum marianum* L. were stirred in NaOH, KOH, and H_3PO_4 to obtain a chemical activation process. The collected samples were washed with distilled water several times to retrieve adherent soil and impurities. Then, it was separated and brought to the laboratory and dried at 75 °C for 48 h. The dried samples (SMB) were prepared with powdered and sieved at 0.2–1 mm in certain proportions as 100 g-portion into plastic containers. The 100 g of rinsed SMB were immersed in aqueous NaOH, KOH, and H_3PO_4 solution (SMB: NaOH, KOH, and H_3PO_4 = 1:1, 2:1, 3:1, 4:1, and 5:1 by mass) and thoroughly stirred for 1 h at room temperature, respectively. Water content was evaporated at 80 °C from each mixture by a temperature controller heater. The dried blends were pyrolyzed in the high-temperature fixed-bed reactor at six different temperatures heated up to 450, 550, 650, 750, 850, and 950 °C in a muffle furnace until 3 h upon a heating rate of 5.0 °C min^{-1} under a nitrogen (N_2) flow rate of 50 mL/min. After the carbonization process, the resulting solid was

repeatedly washed with 0.1, 0.5, and 1 M HCl for activation with KOH and NaOH for activation with H_3PO_4 and deionized water until the pH value of filtrate reached neutral for dissolving ash and inorganic salts. The SMACs were dried at 80 °C for 24 h. More detailed preparation of activated carbon and carbonization procedure were published in a separate study [37]. For higher styrene adsorption, 3 samples with high capacities were determined among 270 carbon samples. The final products are referred to as SMAC1 and SMAC270.

2.2 SMACs properties

The proximate SMB and SMACs were analyzed using ASTM D 3172–3175 methods [38]. Textural properties of the SMB and SMACs were measured using the elemental analyzer (Eurovector, EA3000-Single) for C, H, N, and O content. The morphologies of the SMACs were obtained utilizing SEM (scanning electron microscopy) brand by FEI Quanta FEG 250 as 15 kV and 1000–10,000×. The functional groups of the SMACs surface were identified using Fourier transform infrared (FTIR) spectroscopy; thoroughly, the SMACs particles were pelleted mixing with KBr (KBr: sample weight ratio = 150:1) by Perkin-Elmer, USA. To measure, the specific surface area (S_{BET}) was determined by N_2 adsorption–desorption analysis, and surface areas of the SMACs were estimated from the BET (Brunauer–Emmett–Teller) Quantachrome NOVAtouch LX4 apparatus (South San Francisco, CA, USA). The micropore and mesopore volume (V_{micro} and V_{meso}) was obtained from the t-plot (Harkins–Jura equation) and the BJH (Barret-Joyner Halenda) models. The devolatilization behavior SMACs were operated underneath high heating rate conditions from 50 to 850 °C with oxygenated conditions rate at 10 °C min^{-1} by STA7300 thermal gravimetric analyzer (TGA, HITACHI).

2.3 Batch adsorption

Batch adsorption experiments of SMAC82, SMAC137, and SMAC249 were conducted at 25, 35, and 45 °C with various initial concentrations altering from 10 to 700 ppm of gas styrene. 750 mg of SMAC82, SMAC137, and SMAC249 were used for 130 min at tested adsorption temperature with a thermostatic controller. Preliminary experiments indicated that this contact time ensured controlled the adsorption equilibrium. Also, any leakage, leakage, or retention rates of the reactor conditions were determined in these preliminary experiments. It is convenient to remark that all these styrenes were present as adhesive molecules in the gas environment at tested operating conditions. After selecting, the loss and adhesion rates were started under these conditions in the experiments. First, SMAC82 was placed, and different initial conditions were loaded into the system. The nine different samples were collected from the reactor for 130 min. These sampling times were taken from 10, 20, 30, 50, 70, 90, 110, and 130 min, respectively. For practical applications, styrene adsorption stability is also critical. Hence, the vacuum air pump (AirChek XR5000 SKC, USA), which helps collect the reactor samples, was adjusted and transferred to Tenax tubes without interruption, according to the US EPA Method TO-17 [39]. Nine sampling tubes were used for each experiment and kept at − 20 °C, closing the mouths tightly until analyzing. TD-GC/MS (Thermal Desorber, Markes Unity)–(Gas chromatography, Thermo Scientific Trace 1300)/(Mass detector, Thermo Scientific ISQ QD) and capillary column (TG-624; 30.0 m × 0.25) used for the analysis of Tenax tubes at the end of the experiments mm × 1.4 µm) having a flow rate of 20.0 mL/min N_2 as carrier gas.

The saturated styrene adsorption capacity was produced from the breakthrough curve using Eq. 1 reported previous study [40].

$$q_{(mg/g)} = \left(\frac{F \times C_0 \times 10^{-9}}{W}\right)\left[\left(\frac{C_i}{C_0} \times t_s\right) - \left(\int_0^{t_s} \frac{C_i}{C_0} d_t\right)\right] \quad (1)$$

This equation shows that q is the saturated styrene sorption capacity (mg/g) and F is the airflow rate (mL/min). The amount of SMACs (g) represents W; C_0 and C_i are styrene inlet and outlet concentration (ppm); and t_s is saturation time (min), respectively.

3 Results

3.1 Surface morphologies of the SMACs

Table 1 presents the structural parameters of the SMAC82, SMAC137, and SMAC249, which were produced carbonaceous porous substances under different conditions. The S_{BET} and V_{pore} of SMAC82, SMAC137, and SMAC249 increased significantly compared to SMB; the specific surface areas of the SMB, SMAC82, SMAC137, and SMAC249 were 2.2, 1013, 809, and 573 m^2/g, respectively. SMAC82 had a high specific surface area; the dominant micropores and substantial pore structures enabled styrene to capture without any structure destruction. SMAC82, SMAC137, and SMAC249 are carbon-based adsorbents with the highest S_{BET} and V_{mic} among the adsorbents produced. In the preparation of SMAC82, after it was made with 4:1 (w/w) KOH at 850 °C carbonization temperature for 3 h, after washing with 0.1 M HCl. SMAC137 was produced with 2:1 (w/w) NaOH at 650 °C carbonization temperature for 2 h, after washing with 1 M HCl. SMAC249 was made with 3:1 (w/w) H_3PO_4 at a carbonization temperature of 750 °C

Table 1 Preparation conditions of SMACs

Preparation circumstances				Textural properties			Labeling of samples ID
Activating agent	Mass ration	Activation conditions	Washing conditions	S_{BET} (m^2/g)	V_t (cm^3/g)	V_{mic} (cm^3/g)	
-	-	-	-	2.2	-	-	SMB
KOH	4:1	850 °C, 3 h	0.1 M HCl	1013	0.48	0.27	SMAC82
NaOH	2:1	650 °C, 2 h	1 M HCl	809	0.33	0.19	SMAC137
H_3PO_4	3:1	750 °C, 2 h	0.1 M NaOH	573	0.24	0.13	SMAC249

Table 2 Proximate and ultimate analysis of SMB and SMACs

AC ID	Ultimate (%)				Proximate (%)				Yield (%)
	C	H	N	O	Moisture	Fixed carbon	Volatile matters	Ash	
SMB	46.47	8.81	1.32	43.4	7.50	20.49	71.86	0.15	-
SMAC82	74.50	3.59	2.49	19.42	3.55	75.30	18.86	2.29	73.8
SMAC137	70.29	4.43	3.20	22.08	3.76	72.22	20.55	3.20	66.2
SMAC249	62.37	5.71	1.73	30.19	2.55	73.47	20.46	3.52	68.7

for 2 h, then washed with 0.1 M NaOH, and dried in an oven at 100 °C for 5 h.

Table 2 shows that the proximate and ultimate analyses were performed in this study. SMB and SMACs contain 7.50 and 2.55–3.76% moisture, 71.86 and 18.86–20.55% volatile content, 0.15 and 2.29–3.52% ash, and 20.49 and 72.22–75.30% fixed carbon. SMAC82 involves low volatile substance (18.86%), low ash contents (3.29%), and a high amount of fixed carbon (75.30%) which gets it a proper precursor compared to SMAC137 and SMAC249. The elemental analysis of SMAC82, SMAC137, and SMAC249 has 74.50, 70.29, and 62.37% C; 3.59, 4.43, and 5.71% H; 2.49, 3.20, and 1.73% N; 19.42, 22.08, and 30.19% O. The results displayed that the SMAC82 has a high amount of carbon, and its yield obtained under optimized conditions was 73.80%

Figure 1 demonstrates the N_2 adsorption isotherms at − 196 °C for SMAC82, SMAC137, and SMAC249. The N_2 molecule's adsorption at low relative pressures in SMB is omissible, which can be evidenced to the extent that there is no porosity due to diffusional problems of N_2 at this temperature. From the N_2 isotherms, the microporous character of SMAC82, SMAC137, and SMAC249 can be overtly remarked in which the sequence of N_2 adsorption capacities is SMAC82 > SMAC137 > SMAC249. Isotherms are type IV and H_4 hysteresis loop, which could be dedicated to the presence of microporous and mesopores with the major N_2 adsorption uptake occurring at relative pressures range $P/P_0 > 0.5$ for the directive of the International Union of Pure and Applied Chemistry (IUPAC), being the adsorption almost constant at higher relative pressures [41]. This outcome evidenced that calcination time is considerable in well-improvement pores of SMAC82 prepared from SMB using KOH.

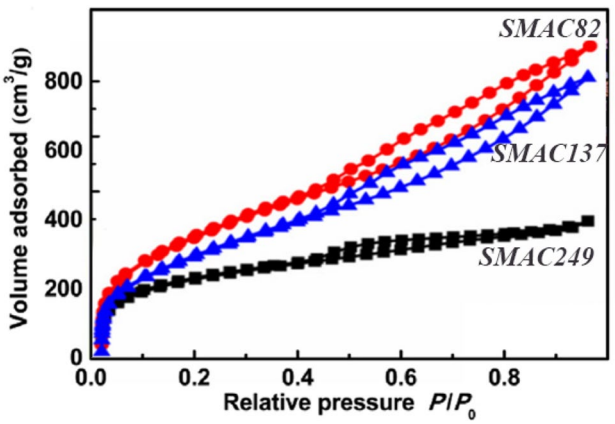


Fig. 1 Adsorption–desorption isotherms of N_2 for SMAC82, SMAC137, and SMAC249

Figure 2 demonstrates the SEM images of SMB, SMAC82, SMAC137, and SMAC249 prepared under optimized conditions. The micrographs of SMB have no cavities, cracks, or crevices, although the surface of the SMAC82, SMAC137, and SMAC249 has rough and porous forms of several dimensions. The excavations were emergent during carbonization due to KOH, NaOH, and H3PO4 activation. In addition, during the calcination operation, the release of large volatile molecules from the surface left behind the porous, rough, and ruptured surface of SMACs. Thus, sights affirm that the SMAC82, SMAC137, and SMAC249 are porous and would be useful adsorbents in the styrene capture mechanism. A similar SEM scene was also observed for carbon-based adsorbent acquired from diverse biowastes [42, 43].

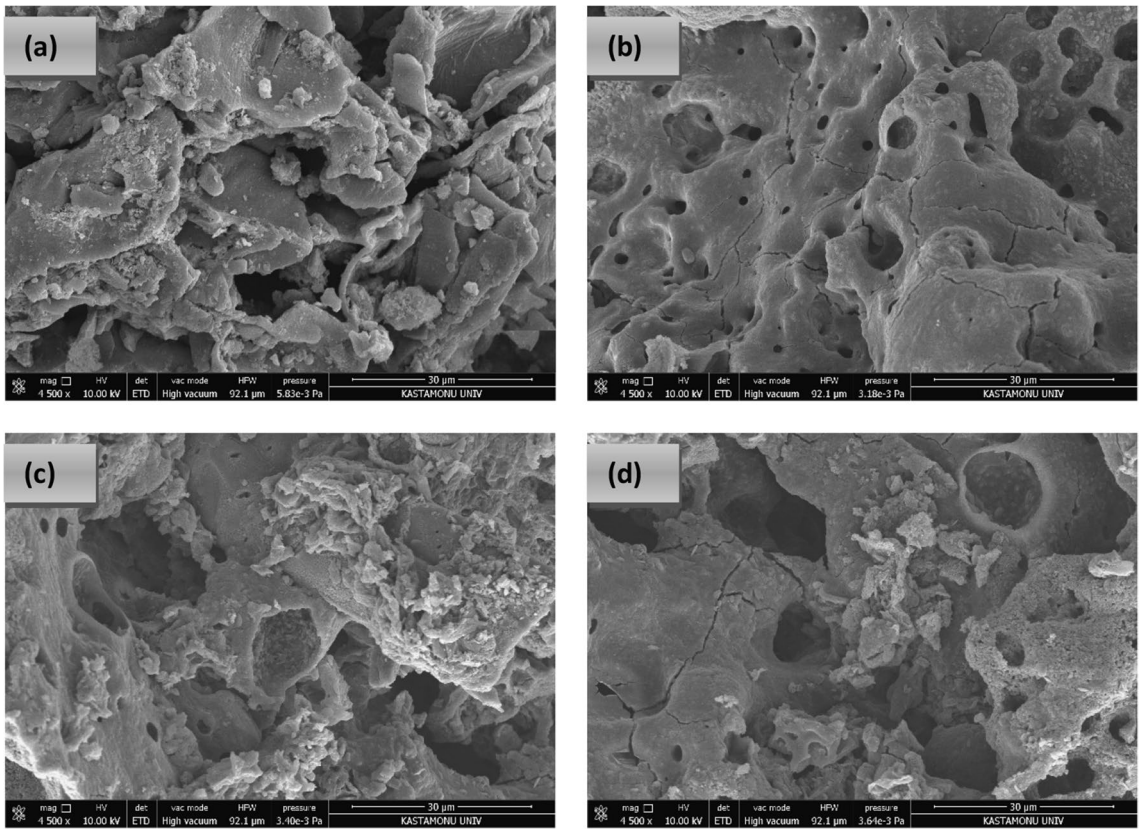


Fig. 2 SEM micrographs of (**a**) SMB, (**b**) SMAC82, (**c**) SMAC137, and (**d**) SMAC249

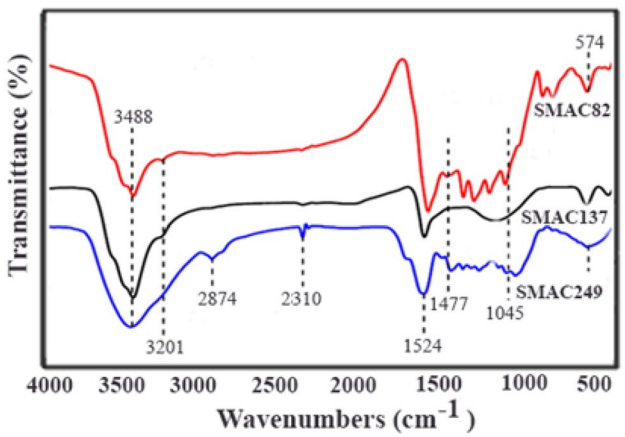


Fig. 3 FT-IR of SMAC82, SMAC137, and SMAC249

The surface chemical properties of SMAC82, SMAC137, and SMAC249 were characterized using FT-IR. Figure 3 displays recorded spectra in the range of 400 to 4000 cm^{-1}. The positions of the absorption peaks of SMAC82, SMAC137, and SMAC249 were roughly the same. Still, the peak intensities were dissimilar, which showed that the functional group's kinds before and after the chemical activation of the SMAC82, SMAC137, and SMAC249 had not altered but that the number had changed as a total of 7 absorption peaks. The broad peak between 3488 and 3201 cm^{-1} represents stretching vibration of O–H bond of cellulose, lignin, and hemicellulose [44], the small peaks at 2874 cm^{-1} correspond to asymmetric C-H vibration (stretching) of the CH_2 moiety existing in lignin, the band located at 2310 cm^{-1} is assigned to the stretching vibration of C = O bond [45], the strong peak at 1524–1477 cm^{-1} might be the bending of C–H [46], and the peak at 1045 cm^{-1} ascribes to the stretching vibration of different C–O bond of lactonic, carboxylic, and alcoholic groups [47]. The broad band centered betwixt 574 and 850 cm^{-1} may have been caused by the out-of-plane bending vibration of the C-H compound [48]. It can be seen that the peak sites of surface functional groups on SMAC82, SMAC137, and SMAC249 are similar for surface functional groups, which indicates that some of the groups are almost the same. However, the contents of surface functional groups may not be alike.

TGA curves have been demonstrated in Fig. 4, which were recorded to assess the thermal stability of SMAC82, SMAC137, and SMAC249 underneath processing temperatures, followed by their dryness at 80 °C for 3 h. The three crucial steps of losing weight were present (i) the

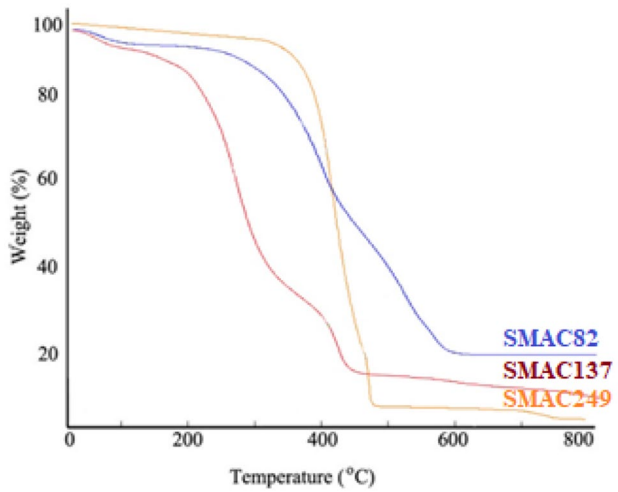


Fig. 4 TGA of SMAC82, SMAC137, and SMAC249

water loss at 100 °C and the first step at 227 °C, which is ingrained in the decomposition of functional moieties on the surface containing oxygen; (ii) the next stage of weight loss, between 285 and 425 °C, is related to decomposing epoxy, hydroxyl, and carboxylic groups in oxygen-containing moieties [49]; (iii) carbon backbone decomposing after 435 °C [50]. The SMB consists of cellulose, hemicellulose, and lignin. Cellulose decomposes in temperatures spanning from 486 to 615 °C.

3.2 Styrene adsorption onto SMACs

3.2.1 Effect of initial concentration

The removal efficiency, loss of efficiency, and resistance to SMAC82, SMAC137, and SMAC249 dosing capacity are given during filtration. While the highest efficiency found in this context is 10 ppm, the limit of the response of the adsorbents varies against increasing concentrations. In particular, it caused significant decreases in yield after 100 ppm and clogged the pores in the structure of adsorbents against 300, 500, and 700 ppm. It caused the styrene molecules in the pores to be more adsorbed and even released. While the highest efficiency was found in 10 ppm, styrene removed with SMAC82, 92%, SMAC137, and SMAC249 yields were 88 and 86%. Yields at 700 ppm dropped significantly and were 24, 21, and 17% for SMAC82, SMAC137, and SMAC249. Moreover, the performance rates were determined at different concentrations with and without the adsorbed amount. They were calculated based on the relevant data from the curve in Fig. 5.

3.2.2 Effect of temperature

In order to analyze the impact of different initial conditions studied in adsorption experiments, 8 different concentration loadings were made in Fig. 6. The effect of styrene concentration from 10 to 700 ppm on SMAC82, SMAC137, and SMAC249 under other conditions was investigated. Due to the different physicochemical properties of different adsorbents, the results obtained varied. However, the point where adsorbents exhibit expected behavior is that the amount adsorbed at 10 ppm is less than when it increases to 700 ppm. Although SMAC82, SMAC137, and SMAC249 had an initial concentration of 10 ppm, the adsorbed at 25 °C was 29, 23, and 17 mg/g; at 700 ppm; it was 228, 170, and 136 mg/g. Although the same adsorbents had an initial concentration of 10 ppm and the amount of adsorbed at 35 °C was 23, 18, and 15 mg/g, it decreased to 199, 144, and 111 mg/g at 700 ppm. In fact, their performance at 45 °C reduces significantly compared to other temperatures, 20, 14, and 11 mg/g at 10 and 700 ppm. There was a decrease up to 166, 117, and 93 mg/g. It was observed that the ambient temperature harmed the amount of adsorption level. The styrene was mainly adsorbed at 25 °C, but with an increase of 10 °C, losses were determined between 11.76 and 21.7% in the adsorption amount depending on the concentration at 25–35 °C. In addition, as the temperature increased, styrene began to desorb from the SMAC82, SMAC137, and SMAC249 until 45 °C and was degraded between 31.03 and 39.13%. These results emerged that the efficiency of SMAC82, SMAC137, and SMAC249 for low-temperature adsorption performance was superb, and the styrene molecules likely played a vital role in the low temperature.

3.2.3 Effect of contact time

To explore the impact of contact time on adsorption capacity was investigated by continuously adjusting the reactor temperature to 25 °C. The residence time, a fundamental parameter of the difference in adsorption capacity, depends on the SMAC82, SMAC137, SMAC249, and the initial styrene concentration at which they are loaded in Fig. 7. The main point of adsorbents, which varied according to the loading level, varied depending on the number of pores and the porosity of the pores. The fast-growing accumulation of styrene in SMAC82, SMAC137, and SMAC249 is responsible for the styrene pressure to micropores. When the media concentration starting from 10 ppm reached 700 ppm, the adsorbents were rapidly filled and adhered to the pores. The micropores were filled, and finally, after 300 ppm, the adsorbents were released into the environment. The values obtained by SMAC82, SMAC137, and SMAC249 for 10 ppm are 29, 23, and 17 mg/g; 54, 43, and 38 mg/g for 20 ppm; 81, 62, and 54 mg/g for 50 ppm; 118, 91, and

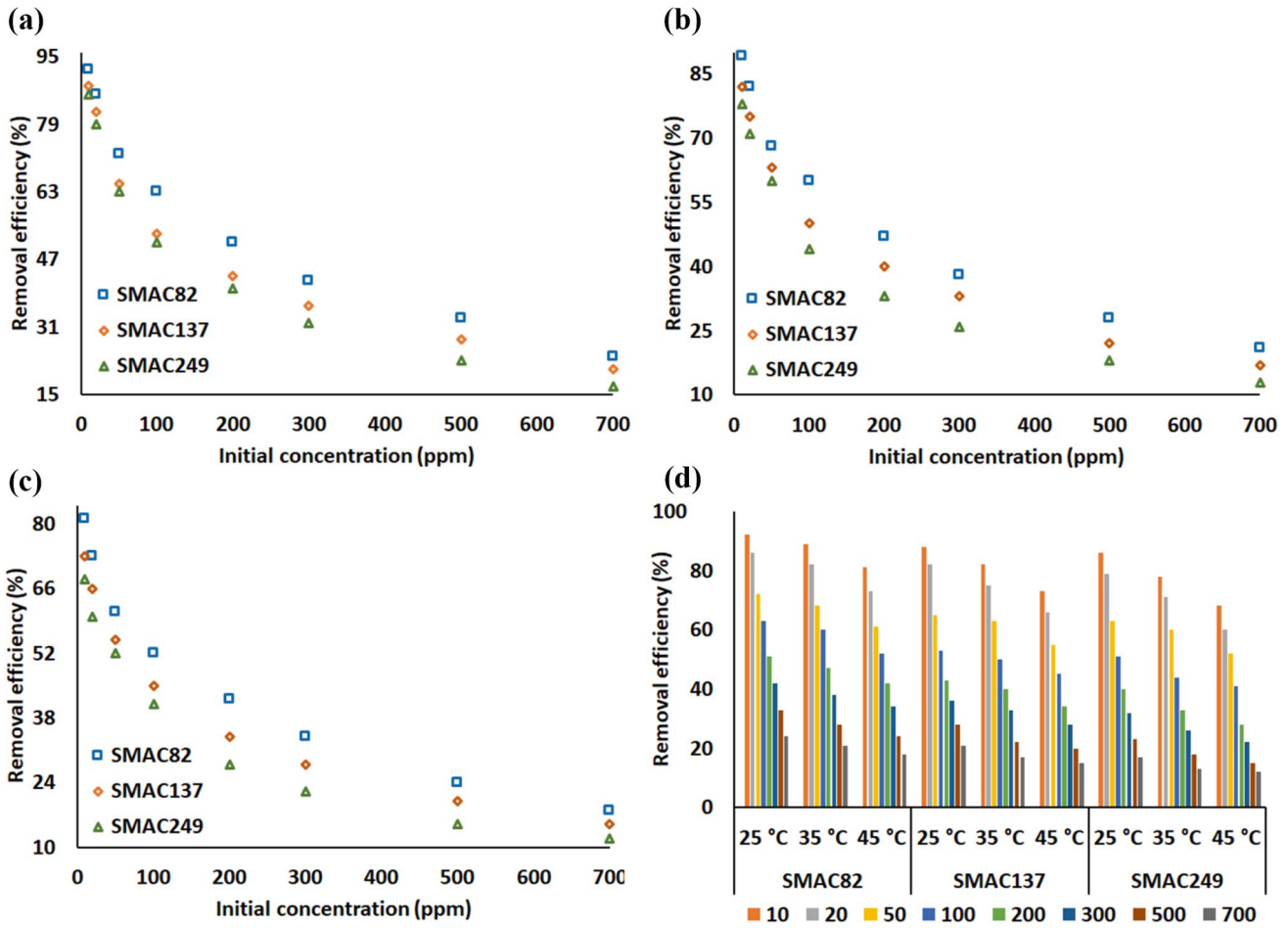


Fig. 5 Removal efficiency (%) based on the initial concentration of **a** 25 °C, **b** 35 °C, **c** 45 °C, and **d** all conditions

76 mg/g for 100 ppm; 165, 129, and 103 mg/g; 204, 157, and 122 mg/g for 300 ppm; 236, 160, and 134 mg/g for 500 ppm; and 229, 170, and 136 mg/g for 700 ppm. As double the initial concentration of 10 ppm, the adsorption amount is 46.30–55.27%; while increasing it 5 times, 62.90–68.52% in adsorption amount. Also, 10 times, the amount of adsorption is 74.73–77.63%; and growing it 30, 50, and 70 times, it is seen that there is no significant increase in the amount of adsorption. The main reasons contribute to a better grasping the adsorbed capacity of SMAC82, SMAC137, and SMAC249 by outlining the probable emphasizing process.

4 Discussion

Styrene poses a severe threat to the ecological environment and human health. It is toxic, carcinogenic, and mutagenic according to the concentration in the ambient air [51, 52]. In addition to harming human health, it contributes significantly to the depletion of the stratospheric ozone layer and regional ozone formation [53]. Adsorption, an effective way, has been used to prevent increased emissions in the indoor environment for VOCs, including styrene, to improve and advance human well-being [54]. In this method, which many researchers use to remove styrene in the gas phase, adsorbents' appropriate production and development have been critical in adsorption efficiency [55, 56]. It is also imperative that the adsorbents produced are environmentally friendly and reusable according to the production method and raw material [57]. To date, styrene has been removed by many different adsorbents [58], including activated carbons (ACs) [59], zeolites [60], hyper-crosslinked polymeric resins (HPR), silica gel [61], metal–organic frameworks (MOFs) [15], and carbon nanotubes [62].

In particular, activated carbons produced from carbon-based lignocellulosic wastes have low cost, easy production, and high holding capacity compared to the activation of adsorbents. It has been stated that VOC adsorption is included in many researchers' studies as physical adhesion. Still, a small amount of chemical bonding can be experienced. Some scientific research on removing styrene from gases uses several adsorbents [63, 64]. Matusik et al. [65]

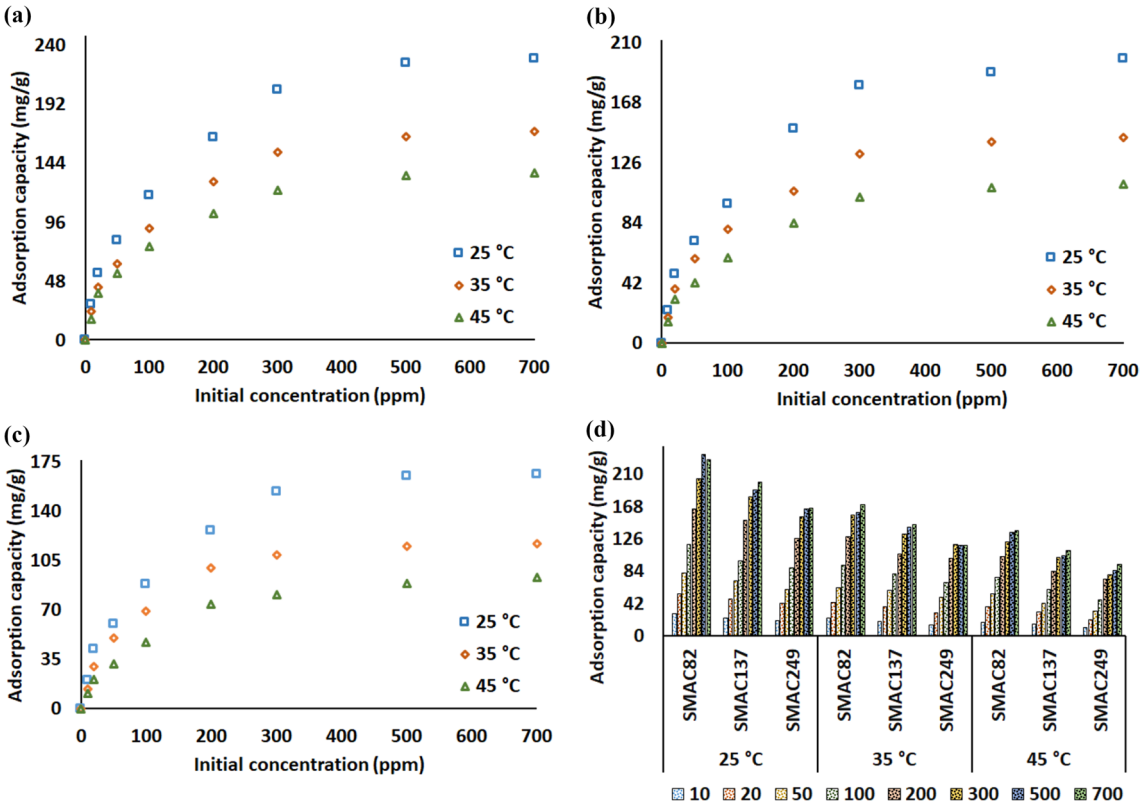


Fig. 6 Adsorption capacity based on the initial concentration of **a** SMAC82, **b** SMAC137, **c** SMAC249, and **d** all conditions

studied gaseous styrene adsorption–desorption efficiency by 18 organosmectites using three host minerals as SWy, STx, and BId (the S_{BET} were from 28 to 127 m^2/g) minerals from ion-exchange method. Like all adsorbents, they have been reported to be highly affected by relative humidity (RH). Thus, the experiments were carried out to improve their adsorption affinity to styrene at RH in the range of 35–55% and at 40 °C. The present study showed that certain adsorbents played a more influential role in styrene removal than each adsorbent produced, thereby in ambient conditions such as RH and temperature. Therefore, the physicochemical structure of the adsorbent produced is important between surfactant molecules and was more available for styrene. Styrene molecules can quickly diffuse and adsorb into mesoporous adsorbents. Duan et al. [66] investigated styrene adsorption capacities using 0.05 g raw sepiolite (the S_{BET}: 29.18 m^2/g and $V_{total:}$ 0.056 cm^3/g) and modified sepiolite (the S_{BET}: 86.66 m^2/g and $V_{total:}$ 0.066 cm^3/g) into the quartz tube reactor. They determined the initial styrene concentration as 14.4 mg/L and reactor temperature at 30, 35, and 40 °C. The maximum styrene adsorption capacity onto the sepiolite was 24 mg/g at 30 °C. In the above-reported studies, the economical production of adsorbent is significant from an adsorption point of VOC application. The amount retained in carbon-based adsorbents is higher than in sepiolite. This finding further confirms the differences between adsorbents [67–69]. These results supported that SMAC82 showed the much better-adsorbed amount of styrene which included decreases as the temperature increases; however, the adsorption capacity does not reduce dramatically. To further discover the intermediates formed over time during styrene adsorption need to determine the correlation between the surface groups on SMAC82 and styrene molecules.

5 Conclusion

Styrene is a component of many chemical substances as reactants and solvents that humans encounter during their occupational and non-occupational environments. It is one of the aromatic hydrocarbon groups used in producing thousands of daily products and causes serious health problems. This study used NaOH, KOH, and H_3PO_4 impregnation to make SMACs derived from biowaste for styrene adsorption under several conditions. Efficiency results show increased styrene adsorption capacity after chemically linking with KOH than NaOH and H_3PO_4 due to increased micropore formation. Adsorption capacities of styrene on SMAC82, SMAC137, and SMAC249 were investigated with different

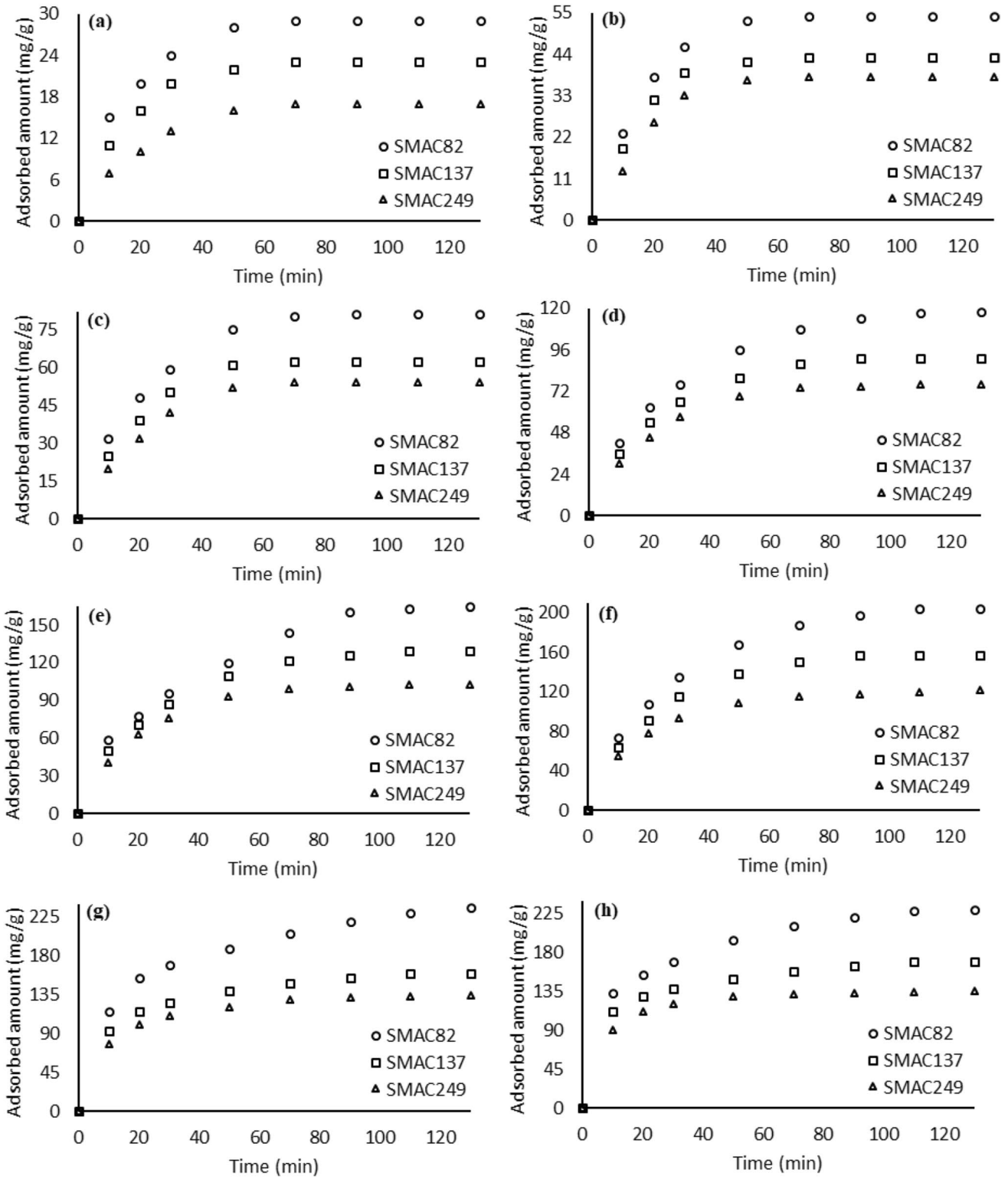


Fig. 7 Effect of contact time on styrene adsorbed amount of **a** 10 ppm; **b** 20 ppm; **c** 50 ppm; **d** 100 ppm; **e** 200 ppm; **f** 300 ppm; **g** 500 ppm, and **h** 700 ppm

initial concentrations. The SMAC82 appears to be the best adsorbent for removing styrene because it has a more surface basic group, larger pore volume, and greater surface area. Experiments results indicated that the efficiency of SMAC82, SMAC137, and SMAC249 for 25 °C adsorption performance was more excellent than 35 and 45 °C, which improved its molecules activities and played a crucial role in the adsorption reaction. To generate a more detailed insight into styrene behavior, further adsorption works to describe certain molecular pathways are required.

Author contribution Kaan Isinkaralar: Investigation, data curation, original draft preparation, writing–reviewing and editing. Kulzira Mamyrbayeva: Investigation, writing—original draft preparation. Ahmad Hosseini-Bandegharaei: Writing—original draft preparation.

Data availability The data that support the findings of this study are available from the corresponding author, upon reasonable request.

Declarations

Ethics approval Not applicable.

Competing interest The author declares no competing interests.

References

1. Wang H, Nie L, Li J, Wang Y, Wang G, Wang J, Hao Z (2013) Characterization and assessment of volatile organic compounds (VOCs) emissions from typical industries. Chin Sci Bull 58:724–730. https://doi.org/10.1007/s11434-012-5345-2
2. Li G, Wei W, Shao X, Nie L, Wang H, Yan X, Zhang R (2018) A comprehensive classification method for VOC emission sources to tackle air pollution based on VOC species reactivity and emission amounts. J Environ Sci 67:78–88. https://doi.org/10.1016/j.jes.2017.08.003
3. World Health Organization (2020) IARC monographs on the identification of carcinogenic hazards to humans. Agents Classified by the IARC Monographs; World Health Organisation: Geneva, Switzerland, 1:125
4. Flaxbart D (1999) Kirk− othmer encyclopedia of chemical technology, 27-Volume Set Wiley Interscience: New York, 1992− 1998
5. Mögel I, Baumann S, Böhme A, Kohajda T, von Bergen M, Simon JC, Lehmann I (2011) The aromatic volatile organic compounds toluene, benzene and styrene induce COX-2 and prostaglandins in human lung epithelial cells via oxidative stress and p38 MAPK activation. Toxicology 289(1):28–37. https://doi.org/10.1016/j.tox.2011.07.006
6. CHCC (2021) Chemicals of high concern to children reporting list Department of ecology State of Washington, United States
7. Pilevar Z, Bahrami A, Beikzadeh S, Hosseini H, Jafari SM (2019) Migration of styrene monomer from polystyrene packaging materials into foods: characterization and safety evaluation. Trends Food Sci Technol 91:248–261. https://doi.org/10.1016/j.tifs.2019.07.020
8. Ajaj A, J'Bari S, Ononogbo A, Buonocore F, Bear JC, Mayes AG, Morgan H (2021) An insight into the growing concerns of styrene monomer and poly (styrene) fragment migration into food and drink simulants from poly (Styrene) packaging. Foods 10(5):1136. https://doi.org/10.3390/foods10051136
9. Chambers DM, Reese CM, Thornburg LG, Sanchez E, Rafson JP, Blount BC, Ruhl JRE, De Jesús IIIR, De Jesús VR (2018) Distinguishing petroleum (crude oil and fuel) from smoke exposure within populations based on the relative blood levels of benzene, toluene, ethylbenzene, and xylenes (BTEX), styrene and 2, 5-dimethylfuran by pattern recognition using artificial neural networks. Environ Sci Technol 52(1):308–316. https://doi.org/10.1021/acs.est.7b05128
10. Farcas MT, Stefaniak AB, Knepp AK, Bowers L, Mandler WK, Kashon M, Jackson SR, Stueckle TA, Sisler JD, Friend SA, Qi C, Hammond DR, Thomas TA, Matheson J, Castranova V, Qian Y (2019) Acrylonitrile butadiene styrene (ABS) and polycarbonate (PC) filaments three-dimensional (3-D) printer emissions-induced cell toxicity. Toxicol Lett 317:1–12. https://doi.org/10.1016/j.toxlet.2019.09.013
11. Tohid L, Sabeti Z, Sarbakhsh P, Benis KZ, Shakerkhatibi M, Rasoulzadeh Y, Rahimian R, Darvishali S (2019) Spatiotemporal variation, ozone formation potential and health risk assessment of ambient air VOCs in an industrialized city in Iran. Atmos Pollut Res 10(2):556–563. https://doi.org/10.1016/j.apr.2018.10.007
12. Banton MI, Bus JS, Collins JJ, Delzell E, Gelbke HP, Kester JE, Moore MM, Waites R, Sarang SS (2019) Evaluation of potential health effects associated with occupational and environmental exposure to styrene–an update. J Toxicol Environ Health Part B 22(1–4):1–130. https://doi.org/10.1080/10937404.2019.1633718
13. Kik K, Bukowska B, Sicińska P (2020) Polystyrene nanoparticles: sources, occurrence in the environment, distribution in tissues, accumulation and toxicity to various organisms. Environ Pollut 262:114297. https://doi.org/10.1016/j.envpol.2020.114297
14. Collins JJ, Delzell E (2018) A systematic review of epidemiologic studies of styrene and cancer. Crit Rev Toxicol 48(6):443–470. https://doi.org/10.1080/10408444.2018.1445700
15. Maes M, Vermoortele F, Alaerts L, Couck S, Kirschhock CE, Denayer JF, De Vos DE (2010) Separation of styrene and ethylbenzene on metal− organic frameworks: analogous structures with different adsorption mechanisms. J Am Chem Soc 132(43):15277–15285. https://doi.org/10.1021/ja106142x
16. Zhang Q, Wang WJ, Lu Y, Li BG, Zhu S (2011) Reversibly coagulatable and redispersible polystyrene latex prepared by emulsion polymerization of styrene containing switchable amidine. Macromolecules 44(16):6539–6545. https://doi.org/10.1021/ma201056g
17. Hou G, Tao W, Liu J, Zhang X, Dong M, Zhang L (2018) Effect of the structural characteristics of solution styrene–butadiene rubber on the properties of rubber composites. J Appl Polym Sci 135(24):45749. https://doi.org/10.1002/app.45749
18. Yao Z, Shen X, Ye Y, Cao X, Jiang X, Zhang Y, He K (2015) On-road emission characteristics of VOCs from diesel trucks in Beijing, China. Atmos Environ 103:87–93. https://doi.org/10.1016/j.atmosenv.2014.12.028
19. Wang Z, Li H, Li T, Zhang Q, Cai Y, Bai H, Lv Q (2023) Application of validated migration models for the risk assessment of styrene and acrylonitrile in ABS plastic toys. Ecotoxicol Environ Saf 252:114570. https://doi.org/10.1016/j.ecoenv.2023.114570
20. Wu X, Li J, Yao L, Xu Z (2020) Auto-sorting commonly recovered plastics from waste household appliances and electronics using near-infrared spectroscopy. J Clean Prod 246:118732. https://doi.org/10.1016/j.jclepro.2019.118732
21. Bhuvaneswari R, Nagarajan V, Chandiramouli R (2021) First-principles research on adsorption properties of o-xylene and styrene on 5–8 phosphorene sheets. Chem Phys Lett 765:138244. https://doi.org/10.1016/j.cplett.2020.138244
22. Mukherjee S, Joarder B, Desai AV, Manna B, Krishna R, Ghosh SK (2015) Exploiting framework flexibility of a metal–organic framework for selective adsorption of styrene over ethylbenzene. Inorg Chem 54(9):4403–4408. https://doi.org/10.1021/acs.inorgchem.5b00206

23. Khabiri B, Ferdowsi M, Buelna G, Jones JP, Heitz M (2020) Simultaneous biodegradation of methane and styrene in biofilters packed with inorganic supports: experimental and macrokinetic study. Chemosphere 252:126492. https://doi.org/10.1016/j.chemosphere.2020.126492
24. Wongbunmak A, Panthongkham Y, Suphantharika M, Pongtharangkul T (2021) A fixed-film bioscrubber of Microbacterium esteraromaticum SBS1–7 for toluene/styrene biodegradation. J Hazard Mater 418:126287. https://doi.org/10.1016/j.jhazmat.2021.126287
25. Huang Q, Zhang H, Xiong L, Huang C, Guo H, Chen X, Luo M, Tian L, Lin X, Chen X (2018) Controllable synthesis of styrene-divinylbenzene adsorption resins and the effect of textural properties on removal performance of fermentation inhibitors from rice straw hydrolysate. Ind Eng Chem Res 57(14):5119–5127. https://doi.org/10.1021/acs.iecr.8b00545
26. Rudra R, Kumar V, Pramanik N, Kundu PP (2017) Graphite oxide incorporated crosslinked polyvinyl alcohol and sulfonated styrene nanocomposite membrane as separating barrier in single chambered microbial fuel cell. J Power Sources 341:285–293. https://doi.org/10.1016/j.jpowsour.2016.12.028
27. Liu H, Xu M, Li G, Zhang W, An T (2021) Solar-light-triggered regenerative adsorption removal of styrene by silver nanoparticles incorporated in metal–organic frameworks. Environ Sci Nano 8(2):543–553. https://doi.org/10.1039/D0EN01011A
28. Runye Z, Christian K, Zhuowei C, Lichao L, Jianming Y, Jianmeng C (2015) Styrene removal in a biotrickling filter and a combined UV–biotrickling filter: steady-and transient-state performance and microbial analysis. Chem Eng J 275:168–178. https://doi.org/10.1016/j.cej.2015.04.016
29. San-Valero P, Gabaldón C, Penya-roja JM, Quijano G (2017) Enhanced styrene removal in a two-phase partitioning bioreactor operated as a biotrickling filter: towards full-scale applications. Chem Eng J 309:588–595. https://doi.org/10.1016/j.cej.2016.10.054
30. Li X, Zhang L, Yang Z, Wang P, Yan Y, Ran J (2020) Adsorption materials for volatile organic compounds (VOCs) and the key factors for VOCs adsorption process: a review. Sep Purif Technol 235:116213. https://doi.org/10.1016/j.seppur.2019.116213
31. Zhu L, Shen D, Luo KH (2020) A critical review on VOCs adsorption by different porous materials: species, mechanisms and modification methods. J Hazard Mater 389:122102. https://doi.org/10.1016/j.jhazmat.2020.122102
32. Choma J, Osuchowski Ł, Dziura A, Marszewski M, Jaroniec M (2015) Benzene and methane adsorption on ultrahigh surface area carbons prepared from sulphonated styrene divinylbenzene resin by KOH activation. Adsorpt Sci Technol 33(6–8):587–594
33. Son HK, Sivakumar S, Rood MJ, Kim BJ (2016) Electrothermal adsorption and desorption of volatile organic compounds on activated carbon fiber cloth. J Hazard Mater 301:27–34. https://doi.org/10.1016/j.jhazmat.2015.08.040
34. Isinkaralar K (2023) Experimental evaluation of benzene adsorption in the gas phase using activated carbon from waste biomass. Biomass Convers Biorefinery 1–10. https://doi.org/10.1007/s13399-023-03979-3
35. Zhang G, Lei B, Chen S, Xie H, Zhou G (2021) Activated carbon adsorbents with micro-mesoporous structure derived from waste biomass by stepwise activation for toluene removal from air. J Environ Chem Eng 9(4):105387. https://doi.org/10.1016/j.jece.2021.105387
36. Isinkaralar K, Turkyilmaz A (2022) Simultaneous adsorption of selected VOCs in the gas environment by low-cost adsorbent from Ricinus communis. Carbon Lett 32(7):1781–1789. https://doi.org/10.1007/s42823-022-00399-7
37. Isinkaralar K (2022) High-efficiency removal of benzene vapor using activated carbon from Althaea officinalis L. biomass as a lignocellulosic precursor. Environ Sci Pollut Res 29(44):66728–66740. https://doi.org/10.1007/s11356-022-20579-2
38. American Society for Testing and Materials (1999) Annual book of ASTM standards: Astm
39. US EPA (1999) Compendium of methods for the determination of toxic organic compounds in ambient air. Center for Environmental Research Information Office of Research and Development, Cincinnati
40. Isinkaralar K (2023) A study on the gaseous benzene removal based on adsorption onto the cost-effective and environmentally friendly adsorbent. Molecules 28(8):3453. https://doi.org/10.3390/molecules28083453
41. Ling LL, Liu WJ, Zhang S, Jiang H (2017) Magnesium oxide embedded nitrogen self-doped biochar composites: fast and high-efficiency adsorption of heavy metals in an aqueous solution. Environ Sci Technol 51(17):10081–10089. https://doi.org/10.1021/acs.est.7b02382
42. Nasrullah A, Saad B, Bhat AH, Khan AS, Danish M, Isa MH, Naeem A (2019) Mangosteen peel waste as a sustainable precursor for high surface area mesoporous activated carbon: Characterization and application for methylene blue removal. J Clean Prod 211:1190–1200. https://doi.org/10.1016/j.jclepro.2018.11.094
43. Isinkaralar K (2022) Theoretical removal study of gas BTEX onto activated carbon produced from Digitalis purpurea L. biomass. Biomass Convers Biorefinery 12(9):4171–4181. https://doi.org/10.1007/s13399-022-02558-2
44. Ogungbenro AE, Quang DV, Al-Ali KA, Vega LF, Abu-Zahra MR (2020) Synthesis and characterization of activated carbon from biomass date seeds for carbon dioxide adsorption. J Environ Chem Eng 8(5):104257. https://doi.org/10.1016/j.jece.2020.104257
45. Bergna D, Varila T, Romar H, Lassi U (2022) Activated carbon from hydrolysis lignin: effect of activation method on carbon properties. Biomass Bioenergy 159:106387. https://doi.org/10.1016/j.biombioe.2022.106387
46. Wu X, Chen L, Chen J, Su X, Liu Y, Wang K, Qin W, Qi H, Deng M (2019) The effect of 60 Co γ-irradiation on the structure and thermostability of alkaline lignin and its irradiation derived degradation products. Waste Biomass Valorization 10:3025–3035. https://doi.org/10.1007/s12649-018-0300-3
47. Zhao J, Xiuwen W, Hu J, Liu Q, Shen D, Xiao R (2014) Thermal degradation of softwood lignin and hardwood lignin by TG-FTIR and Py-GC/MS. Polym Degrad Stab 108:133–138. https://doi.org/10.1016/j.polymdegradstab.2014.06.006
48. Ren Z, Jia B, Zhang G, Fu X, Wang Z, Wang P, Lv L (2021) Study on adsorption of ammonia nitrogen by iron-loaded activated carbon from low temperature wastewater. Chemosphere 262:127895. https://doi.org/10.1016/j.chemosphere.2020.127895
49. Kim BC, Park SW (2008) Fracture toughness of the nano-particle reinforced epoxy composite. Compos struc-tures 86(1–3):69–77. https://doi.org/10.1016/j.compstruct.2008.03.005
50. Kou L, Gao C (2011) Making silica nanoparticle-covered graphene oxide nanohybrids as general building blocks for large-area superhydrophilic coatings. Nanoscale 3(2):519–528. https://doi.org/10.1039/C0NR00609B
51. Shareefdeen Z (2005) Biotechnology for odor and air pollution control. Springer Science & Business Media
52. Farrelly TA, Shaw IC (2017) Polystyrene as hazardous household waste. Household hazardous waste management. InTech
53. Ma Y, Fu S, Gao S, Zhang S, Che X, Wang Q, Jiao Z (2021) Update on volatile organic compound (VOC) source profiles and ozone formation potential in synthetic resins industry in China. Environ Pollut 291:118253. https://doi.org/10.1016/j.envpol.2021.118253
54. Wang H, Ji Y, Chen J, Li G, An T (2015) Theoretical investigation on the adsorption configuration and• OH-initiated photocatalytic degradation mechanism of typical atmospheric VOCs styrene onto (TiO2) n clusters. Sci Rep 5(1):15059. https://doi.org/10.1038/srep15059

55. Zhou DD, Chen P, Wang C, Wang SS, Du Y, Yan H, Ye ZM, He CT, Huang RK, Mo ZW, Huang NY, Zhang JP (2019) Intermediate-sized molecular sieving of styrene from larger and smaller analogues. Nat Mater 18(9):994–998. https://doi.org/10.1038/s41563-019-0427-z
56. Liu R, Song H, Li B, Li X, Zhu T (2021) Simultaneous removal of toluene and styrene by non-thermal plasma-catalysis: effect of VOCs interaction and system configuration. Chemosphere 263:127893. https://doi.org/10.1016/j.chemosphere.2020.127893
57. Albo Hay Allah MA, Alshamsi HA (2023) Facile green synthesis of ZnO/AC nanocomposites using Pontederia crassipes leaf extract and their photocatalytic properties based on visible light activation. J Mater Sci: Mater Electron 34(16):1263. https://doi.org/10.1007/s10854-023-10636-y
58. Koizumi Y, Jin X, Yatabe T, Miyazaki R, Hasegawa JY, Nozaki K, Mizuno N, Yamaguchi K (2019) Selective synthesis of primary anilines from NH3 and cyclohexanones by utilizing preferential adsorption of styrene on the Pd nanoparticle surface. Angew Chem Int Ed 58(32):10893–10897. https://doi.org/10.1002/anie.201903841
59. Isinkaralar K, Meruyert K (2023) Adsorption behavior of multicomponent btex on the synthesized green adsorbents derived from Abelmoschus esculentus L. waste residue. Appl Biochem Biotechnol 195(8):4864–4880. https://doi.org/10.1007/s12010-023-04556-0
60. Ali Rangkooy H, Pour MN, Dehaghi BF (2017) Efficiency evaluation of the photocatalytic degradation of zinc oxide nanoparticles immobilized on modified zeolites in the removal of styrene vapor from air. Korean J Chem Eng 34:3142–3149. https://doi.org/10.1007/s11814-017-0174-2
61. Hou S, Huang ZH, Zhu T, Tang Y, Sun Y, Li X, Shen F (2023) Adsorption removal of styrene on C-Cl grafted silica gel adsorbents. Chemosphere 315:137679. https://doi.org/10.1016/j.chemosphere.2022.137679
62. De Falco A, Marzocca AJ, Corcuera MA, Eceiza A, Mondragon I, Rubiolo GH, Goyanes S (2009) Accelerator adsorption onto carbon nanotubes surface affects the vulcanization process of styrene–butadiene rubber composites. J Appl Polym Sci 113(5):2851–2857. https://doi.org/10.1002/app.30261
63. Onuki S, Koziel JA, Jenks WS, Cai L, Rice S, van Leeuwen JH (2015) Ethanol purification with ozonation, activated carbon adsorption, and gas stripping. Sep Purif Technol 151:165–171. https://doi.org/10.1016/j.seppur.2015.07.026
64. Rangkoy HA, Nakhaei M, Jahani F, Salari S, Nematpour L, Fouladi B (2018) Effect of nano-TiO2 immobilized on activated carbon, zeolite Y and ZSM-5 on the removal of styrene vapors from polluted air. J Nanostruct 8(3):307–315. https://doi.org/10.22052/JNS.2018.03.011
65. Matusik J, Koteja-Kunecka A, Maziarz P, Kunecka A (2022) Styrene removal by surfactant-modified smectite group minerals: efficiency and factors affecting adsorption/desorption. Chem Eng J 428:130848. https://doi.org/10.1016/j.cej.2021.130848
66. Duan E, Han J, Song Y, Guan Y, Zhao W, Yang B, Guo B (2013) Adsorption of styrene on the hydrothermal-modified sepiolite. Mater Lett 111:150–153. https://doi.org/10.1016/j.matlet.2013.08.079
67. Salman NS, Alshamsi HA (2022) Synthesis of sulfonated polystyrene-based porous activated carbon for organic dyes removal from aqueous solutions. J Polym Environ 30(12):5100–5118. https://doi.org/10.1007/s10924-022-02584-1
68. Ali A, Khan S, Ali N, Khan MA (2023) Enhanced ultrasonic adsorption of pesticides onto the optimized surface area of activated carbon and biochar: adsorption isotherm, kinetics, and thermodynamics. Biomass Convers Biorefinery 1–16. https://doi.org/10.1007/s13399-023-04170-4
69. Khalid W, Cheng CK, Liu P, Tang J, Liu X, Ali A, Shahab A, Wang X (2022) Fabrication and characterization of a novel Ba2+-loaded sawdust biochar doped with iron oxide for the superadsorption of SO42− from wastewater. Chemosphere 303:135233. https://doi.org/10.1016/j.chemosphere.2022.135233

Publisher's note Springer Nature remains neutral with regard to jurisdictional claims in published maps and institutional affiliations.

Springer Nature or its licensor (e.g. a society or other partner) holds exclusive rights to this article under a publishing agreement with the author(s) or other rightsholder(s); author self-archiving of the accepted manuscript version of this article is solely governed by the terms of such publishing agreement and applicable law.